Design and testing of a cost-effective active force sensor with servo control

Servo kontrollü maliyet etkin bir aktif kuvvet duyargası tasarımı ve denenmesi

Author (*Yazar*): Kemal YAMAN

ORCID: 0000-0003-3063-391X

Design and Testing of A Cost-effective Active Force Sensor with Servo Control

Highlights

❖ *Cost-effective active suspension system*
❖ *Force sensor*
❖ *Electro-hydraulic servo valves*
❖ *Proportional control*
❖ *Pulse-width modulated signal*

Graphical Abstract

Within the scope of this, a cost-effective force sensor was designed by integrating a compression spring and a linear variable differential transformer (LVDT). The integrated system converts externally applied forces, provided by a force measurement and feedback unit, into electrical signals through the LVDT brush movement
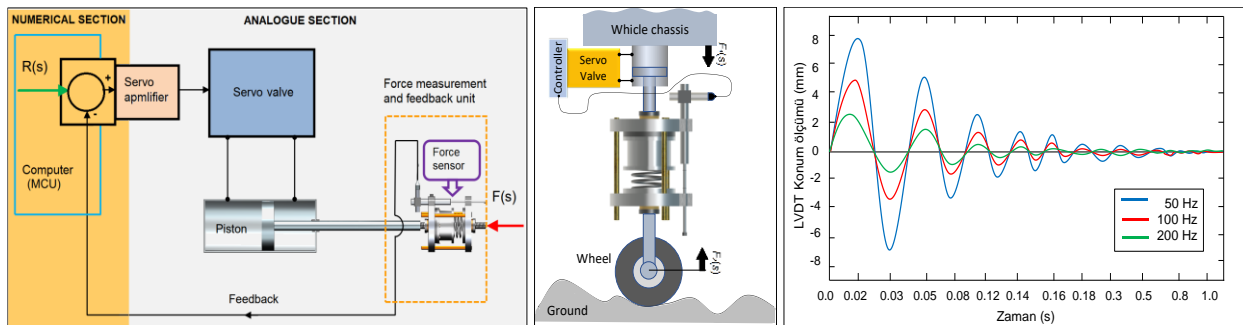
Figure. The designed active force sensor system and its performance

Aim

Developing a cost-effective computer-controlled active suspension system

Design & Methodology

Experimentally worked. For this purpose, an active force measurement sensor was designed, manufactured and integrated into the system. A software was developed and tested for the control of the entire system in a computer environment.

Originality

A cost-effective active suspension system has been developed. A new control software was developed according to an algorithm suitable for the designed system. The developed hydraulic system can be easily converted to a pneumatic system.

Findings

A cost-effective servo-controlled force sensor, utilizing a PWM digital hydraulic position control system, demonstrates successful precision force control over position. This active servo force mechanism relies on impact frequency as a key parameter. The implementation of a PWM hydraulic control system using a digital electro-hydraulic servo system achieves accurate force control based on position. Additionally, the developed hydraulic system can be easily converted to a pneumatic system through control coefficient adjustments.

Conclusion

The study developed a cost-effective force sensor with precise control using a pulse-width modulated (PWM) hydraulic system. While effective at high frequencies (200 Hz), it exhibited oscillations at low frequencies (10-15 Hz). The sensor can be adapted for active suspension in high-speed trains and vehicles. The research underscores the importance of isolating vibrations for accurate results. Overall, the study successfully implemented a PWM hydraulic control system, with potential applications in active suspension and adaptability to a pneumatic system for various industries.

Declaration of Ethical Standards

The author of this article declares that the materials and methods used in this study do not require ethical committee permission and/or legal-special permission.

Design and Testing of a Cost-effective Active Force Sensor with Servo Control

Research Article / Araştırma Makalesi

Kemal YAMAN[1]*

[1]Department of Industrial Design, Architecture and Design Faculty, OSTIM Technical University, 06374, Ankara, Türkiye

(Geliş/Received : 04.08.2023 ; Kabul/Accepted : 27.11.2023 ; Erken Görünüm/Early View : 28.02.2024)

ABSTRACT

In this work, computer-controlled regulation of a hydraulic system with analog features was investigated, and a new force sensor was designed within this scope. The system consists of two main structures: an analog subsystem comprising a four-way servo valve, hydraulic piston, servo amplifier, the designed force sensor and a digital subsystem responsible for comparison and control from a desktop computer. Within the scope of this study, a low-cost force sensor was designed by integrating a compression spring, guides, a support frame, and a Linear Variable Differential Transducer (LVDT). In this integrated system, a force applied at a specific magnitude and frequency from an external force measurement and feedback unit is converted into electrical signals through the horizontal movement of the LVDT core. The analog voltage signals generated by the core are digitized and fed back to the computer and data acquisition card. The digitized data transferred to the developed software in this study continuously ensures position-dependent force control by comparing it with reference data. Experiments conducted with the force sensor placed between two hydraulic pistons controlled by a servo valve demonstrated the system's ability to achieve the desired control by causing the pistons to move right and left in response to reference force input, particularly showing improved stability at high-frequency signal inputs.

Keywords: Active control, active suspension, linear transducer, position control, servo valve, load cell.

Servo Kontrollü Maliyet Etkin bir Aktif Kuvvet Duyargası Tasarımı ve Denenmesi

ÖZ

Bu çalışmada, analog özelliklere sahip bir hidrolik sistemin bilgisayar kontrollü kontrolü incelenmiş ve bu kapsamda yeni bir kuvvet duyargası tasarlanmıştır. Sistem dört yollu servo valf, hidrolik piston, servo yükseltici ve tasarlanan kuvvet duyargasından oluşan analog alt sistem ve masaüstü bilgisayardan oluşan karşılaştırma ve kontrolden sorumlu sayısallaştırıcı alt sistem olmak üzere iki ana yapıdan oluşmaktadır. Bu çalışma kapsamında, bir sıkıştırma yayı, kılavuzlar, bir destek çerçevesi ve bir lineer değişken diferansiyel transdüser (LVDT) entegre edilerek düşük maliyetli bir kuvvet duyargası tasarlanmıştır. Bu entegre sistemde, harici bir kuvvet ölçüm ve geri besleme ünitesinden belirli bir büyüklük ve frekansta uygulanan kuvvet, LVDT çekirdeğinin yatay hareketi ile elektrik sinyallerine dönüştürülür. Çekirdeğin oluşturduğu analog voltaj sinyalleri sayısallaştırılarak bilgisayara ve veri toplama kartına geri beslenir. Bu çalışmada geliştirilen yazılıma aktarılan sayısallaştırılmış veriler, sürekli olarak referans verilerle karşılaştırılarak konuma bağlı kuvvet kontrolü sağlar. Bir servo valf tarafından kontrol edilen iki hidrolik piston arasına yerleştirilen kuvvet duyargası ile yapılan deneyler, pistonların sağa ve sola hareket etmesine neden olarak referans kuvvet girişi ile sistemin istenilen kontrolünü sağladığını ortaya koymuştur. Özellikle yüksek frekanslı sinyal girişlerinde sistemin çok daha kararlı çalıştığı gözlemlendi.

Anahtar Kelimeler: Aktif kontrol, aktif süspansiyon, lineer transdüser, pozisyon kontrol, servovalf, yük hücresi.

1. INTRODUCTION

In today's industry, transportation, medicine, and many other fields, there are small and precise systems that need to establish a connection between humans and machines for various purposes. These small and precise systems play a much more important and valuable role than the large and powerful systems they manage. This is because if the control of these powerful systems is lost, they may not be used as intended and their benefits can turn into harm [1-2]. In fluid power control systems, small units can transfer large powers to the controlled load, and these powers can be easily and precisely controlled within wide limits using valves. These systems can apply high forces and moments to the load with low power loss. They have high response speeds and are less affected by load changes. Moreover, the fluid passing through the system serves as a coolant, removing the heat generated during operation. Simple pressure limiters can be used to protect the system against overload. For these reasons, fluid power control systems are preferred in many applications [3, 4].

Keleş and Ercan [5] investigated the open-loop and closed-loop behavior of a pulse-width-modulated hydraulic system using a combination of theoretical and experimental investigations. Initially, they formulated a mathematical model for the system and devised innovative approaches to derive their response under pulse-width modulated inputs. They then rigorously

Sorumlu Yazar (Corresponding Autho)
e-mail : kemal.yaman@ostimteknik.edu.tr

evaluated the response of servo valve, open-loop and closed-loop hydraulic systems when subjected to pulse-width modulated step and sinusoidal inputs. In particular, they also investigated the effect of pulse frequency on the sinusoidal response. To facilitate their experiments, a comprehensive test setup consisting of a PC, a pulse width modulator, a servo valve-driven hydraulic system and controller feedback elements was meticulously put together. The similar setup was used in the study of Usta [6]. In both studies, experiments have shown that precise position control can be successfully achieved in electro-hydraulic control systems using pulse-width modulated inputs. Furthermore, these studies highlighted that the pulse frequency is the most crucial parameter in a pulse-width-modulated hydraulic system.

Priyandoko et al. [7] investigated the application of adaptive neuro-active force control to a quarter car model with an active vehicle suspension system. They installed an LVDT (linear variable differential transformer) to measure displacements in the suspension system, positioned between the sprung and unsprung masses. The designed neuro-active suspension system was found to outperform the PID controller and passive suspension. Fateh and Allavi [8] presented an innovative approach to enhance the dynamic performance of a vehicle suspension system using impedance control. They employed a hydraulic actuator to counteract road disturbances and regulate the vehicle's behavior. The proposed system comprised two inner loops: a force controller relying on feedback linearization and a position controller employing fuzzy logic. These loops worked in tandem to achieve effective control over the suspension system, delivering a smoother and more stable ride experience in the face of varying road conditions. Their experiments reported that the control system provided much better vibration isolation compared to the passive system. In their study, Wu et al. [9] introduced an innovative force-tracking electro-hydraulic actuator design. Through simulations and experiments, they successfully showcased its excellent performance in dynamic force tracking, meeting all design requirements set by their integrated design methodology. Furthermore, their experiments confirmed the feasibility of the semi-closed loop force control strategy. Jian-ying Li et al. [10] implemented force control in their electro-hydraulic force servo control system using both fuzzy logic and PID control. They found that PID control yielded better results compared to fuzzy logic. Jianying Li et al. [11] conducted a study on an electro-hydraulic load simulator based on simultaneous force control with a dual-piston servo valve arrangement. When the dual servo valve simultaneous control method was applied to the load system, a significant reduction in output force error was observed. In another experimental study conducted by Chen et al. [12], similar to the present study, they investigated the behavior of the system compared to adaptive and PID control by placing a commercial load cell and an LVDT for position control between two bidirectional electro-

hydraulic valves. The designed system demonstrated superior performance in adaptive control compared to PID control when subjected to a sinusoidal signal input. Fu et al [13] examined two different controls of a three-phase electro-hydraulic servo valve as proportional open control and proportional-velocity feedback. By deriving the mathematical model of the system, they theoretically examined the behavior of the dynamic character according to open proportional control and closed loop proportional-speed control. As a result, they showed that the closed loop is more stable than the open proportional loop. Apart from this, there are different applications of electro-hydraulic servo systems according to very different controllers in the literature. For example, Feng et al. [14] studied the control of an excavator arm containing an electro-hydraulic servo valve with an adaptive sliding mode controller based on artificial neural networks (ANN). They reported that with this system they used, they reduced non-linear vibration and unstable movements during the operation of the excavator arm. Coşkun and İtik [15] examined the control behavior of an electro-hydraulic servo valve with an intelligent PID (i-PID) controller, which they designed, according to ramp and sinusoidal disturbance inputs. When they tested the uncertainties and distortion effects of the servo valve model, they used in the studies with i-PID, they observed that the system gave better monitoring results against uncertainties and external factors. Similar to this study, Yang and Yeo [16] studied force control by placing a mass between two electro-hydraulic servo valves. In their study, they monitored the high and low frequency force tracking behavior by means of an encoder integrated with the multilayer ANN controller they developed as the controller and the electro-hydraulic load simulator. They reported that the designed smart controller significantly improved the resulting control performance Çakan et al [17] used the BEES Algorithm to determine the simulation parameters of the MOOG brand D675 series proportional servo valve system. They considered the dynamic properties that best matched the manufacturer's provided data set. It has been shown that the Bees Algorithm (BA) can be used as a fast and reliable way to determine unknown parameters in modeling proportional electro-hydraulic servo valve systems.

Gao et al [18] examined the stability of a similar servo system according to the Gray Wolf optimization algorithm in their theoretical study. They reported that the developed algorithm offers good control performance.

Within the scope of this study, the computer control of an analog hydraulic system has been designed and tested by setting up the system on a workbench. Hydraulic control systems are used in various industrial fields due to their superior features, such as rapid response and the ability to apply high forces. The aim of this study is to develop an experimental hydraulic drive system that can be controlled digitally through a Personal Computer (PC) and a connected servo force mechanism. In practice, such

systems are used in the sensitive suspensions of high-speed trains, as well as in various machines and systems that require force control. In this study, in the initial stage, similar systems and the load cells and other components used in these systems were examined to design a force measurement and feedback system for such an active suspension system.

2. MATERIAL AND METHOD

The electro-hydraulic servo valves used in this system consist of a torque or force motor and one or more stages of control valves driven by it. The servo valve is the highest gain element in the control loop. The control input is an electric current on the order of mA. Its output is the flow provided to the load at a certain load pressure differential. The torque motors driving the servo valve used in the experiments are generally electromechanical devices contained within the servo valve itself. They apply a moment or force proportional to the input current i(t) they receive to the pilot stage, spool, poppet, or jet pipe of the servo valve. In this system, a MOOG 931 model servo valve with a moving coil and an operating frequency between 200-500 Hz was used. The maximum operating pressure of the valve is 200 bar, but for compatibility with other components, it was operated at 100 bar during the experiments. The maximum input current and the flow rate under zero load pressure are 125 cm/s.
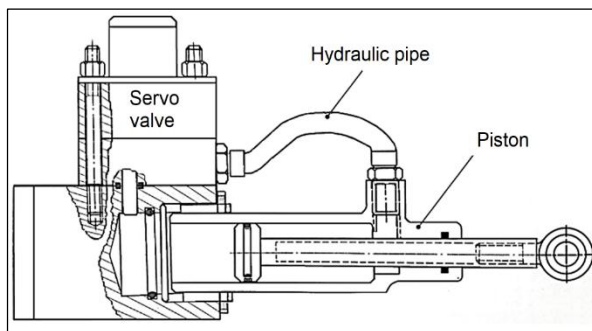
Figure 1. Schematic drawing of the hydraulic piston with servovalve used in the experiments

The established control system was powered by a hydraulic power unit available in the automatic control laboratory. This power unit consists of a pressure-compensated variable-displacement hydraulic oil pump with a piston and a 22 kW electric motor driving it. The pump's output pressure can be manually adjusted up to 200 bars. When the electric motor connected to the hydraulic reservoir operates at a speed of 1450 RPM and the output pressure is set to 200 bars, the pump's flow rate has been measured to be approximately 60 liters per minute. Since the usage pressure of many hydraulic system components used in the experiments is 100 bar, a source pressure of 100 bar was preferred during the experiments. A proportional control, voltage input, and current output DC servovalve amplifier capable of

adjusting proportional gain was used as the servo amplifier. The servovalve amplifier can be adjusted for gain (can operate continuously in the range of 5-190 mA/V). In order to achieve large amplitude position changes during the experiments, the smallest area cylinder available in the laboratory was selected. The selected cylinder has a double-ported single-rod piston. Figure 1 shows a schematic drawing of the hydraulic piston with a servo valve used as the actuator in the experiments. The hydraulic cylinder used for disturbance inputs has the same type and specifications as the main hydraulic system. These specifications can be listed as follows: piston diameter is 24 mm, piston rod diameter is 12.8 mm, and the stroke is 71.2 mm. Accordingly, the area on the side without the piston rod is 445 mm², and on the other side, it is 318 mm².
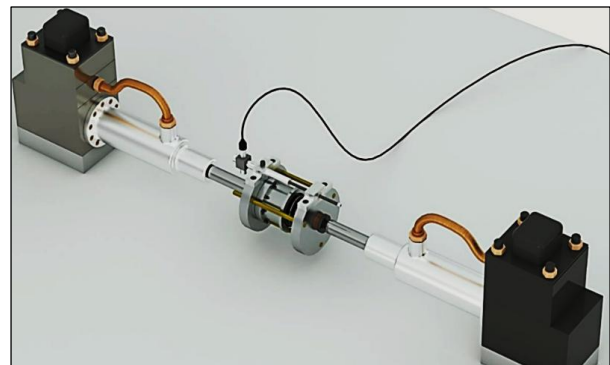
Figure 2. Designed force sensor system and experimental setup

In this study, two different position transducers (LVDTs) were used at different locations in the system, one for providing the disturbance input and the other for force measurement. For the disturbance input system, a SENSOTEC brand, MDL 3000 Model, DCDT type position transducer was used. This transducer has a stroke of ±3 inches, and the transducer coefficient Kt is 1.716 V/inch = 0.06768 V/mm. The position transducer used for force measurement is an HBM (Hottinger Baldwin Messtechnik) brand W20 model. This transducer has a stroke of ±2 cm (or totally 4 cm) and a K value of 2.5 Volt/cm. The system used a standard PC with 8 GB memory and four cores. A digital data acquisition and control card, DAS-20 (Keithley Metrabyte) type, with a total of 16 channels, 8 inputs, and 8 outputs, was connected to the PC via the RS232 port. Each channel of the DAS-20 card can measure a maximum voltage of ±10V. The card can operate in 7 different measurement ranges with gain settings ranging from 0.5 to 100, and the measurement ranges vary between ±10V and ±50 V. In the widest range, the ±10V range, each bit corresponds to 4.88 mV, and in the narrowest range, the ±50mV range, each bit corresponds to 24.4μV. The DAS-20 card has two analog output channels capable of providing voltage in 3 different ranges. Each channel can operate in the range of 0 to +10V, ±10V, or ±5V. The sensitivity of these output voltages is 1/4096. In the ±10V range, each bit

corresponds to 4.38 mV, and in the ±5V or 0 to +10V range, each bit corresponds to 2.44 mV. The maximum current that the analog output channels can provide is 5mA. Since this current is not enough to drive the valve, a servo amplifier is required. Additionally, the maximum 10V voltage of the analog output also necessitates the use of a servo amplifier because the drive power provided by a maximum of 10V voltage and 5mA current is quite low. The user manual that came with the data acquisition and control card is compatible only with programs written in the Microsoft Visual Basic 5.0 coding structure [19].

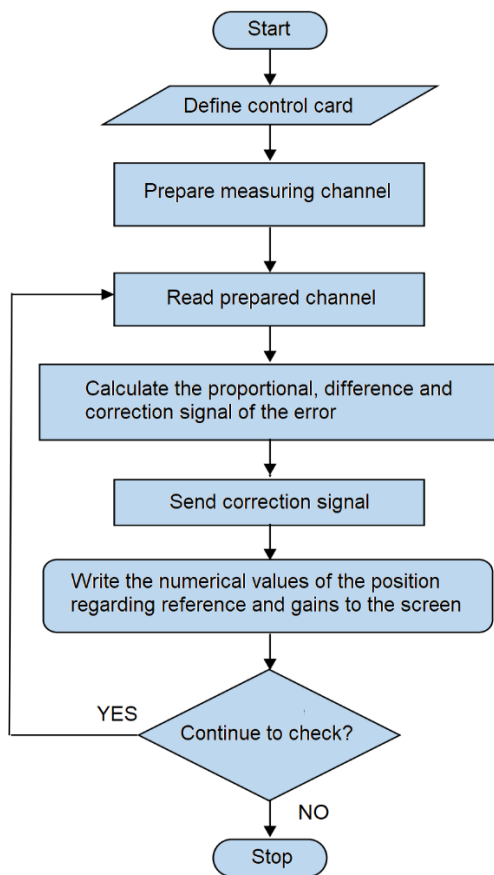The program algorithm is given in Fiğ. 3.

Figure 3. PKON Program algorithm

Therefore, the control program was developed in this programming language and named "PKON." The "PKON" control program is based on proportional control and has a user interface that allows the user to enter the reference value as a digital and step input from the keyboard. The program is compatible with single-channel (or single-axis) input/output. The sampling rate of the "PKON" program was set to approximately 400 levels per second. If the program is converted to the "EXE" extension, this rate can reach up to 500-700 samples per second.

 In this study, the linear variable differential transducer (LVDT) and the components of the designed force transducer system are shown in Fig. 4. All mechanical productions were manufactured using Machining

methods and assembled. Except for the bolts (DIN 912 M8-socket head cap screws) and LVDT, almost all components were made from 7075 aluminum alloy material (AA 7075 T6). As seen in the figure, the LVDT is fixed to the "Front connection plate" part using the "Fastening bolt." On the opposite side, the LVDT core is supported on the "LVDT core holder" part and "Front connection plate rear" platform with the help of "Front bearing" and "Rear bearing" parts.
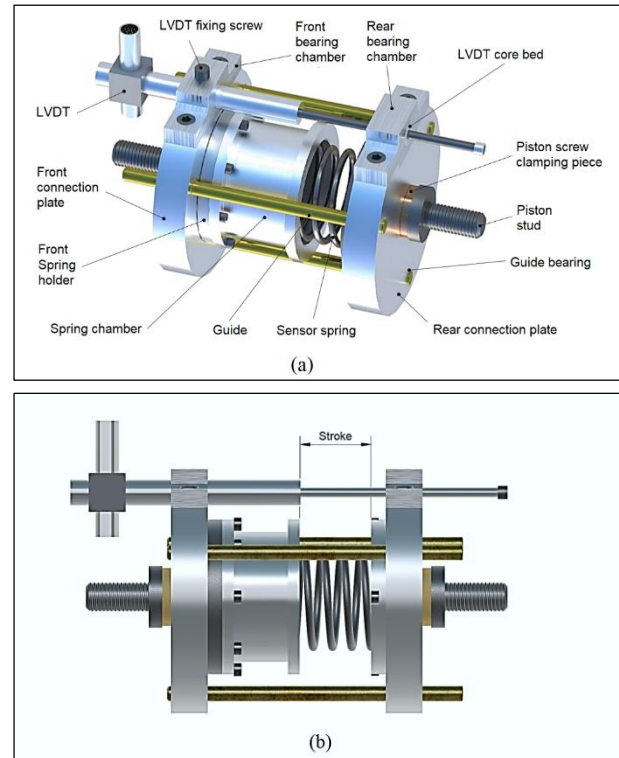

Figure 4. The designed force sensor system includes (a) components and (b) stroke length

The front and rear connection plates are connected to each other using three "Guide" parts made from brass (SAE 17660) material, produced with the turning operation (distributed at 120 degrees). To isolate the vibrations occurring during the movement of the hydraulic pistons, the piston screws are connected to each other using two "Piston screw clamping parts" made from copper material (DIN 1787) and attached to the connection plates. Inside the system, the "Spring holder" and "Spring chamber" parts flexibly connect both connection plates together. This allows the front and rear connection plates, along with the load cell spring, to move forward and backward together with the guides. This movement can be up to the LVDT stroke length. The system is equipped with hydraulic servo-valved pistons on both ends (see Fig. 2). The LVDT is connected to the computer's parallel port through a female connector-cable and is linked to an analog-to-digital converter card.

Here, LVDT Connection plate front, Spring holder, Spring chamber, Guide, Load cell spring, Connection plate rear, Guide bearing, Piston screw, Piston screw

clamping piece, LVDT brush bearing, Rear bearing, Front bearing were tightened with appropriate torque values so that they can withstand the forces generated during operation and remain in their current positions precisely. In addition, the LVDT whole was fixed by tightening the fixing screw (M6) with the appropriate torque, ensuring its horizontal linearity with the help of a comparator. The hydraulic drive pistons are rigidly attached to the table by placing silicone rubber (insulation rubbers) between them by pulling method using four M8 bolts from the bottom on the metal table.
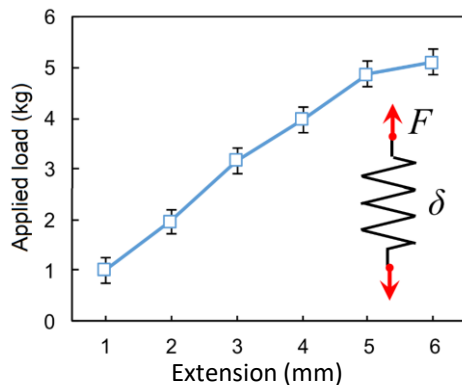
Figure 5. The applied load-extension variation of the compression spring used in experiments

The compression spring used in the experiments is a spring made of SAE 1070 (Ck 67) Spring Steel with a wire diameter of 3 mm, a diameter of 52 mm and a pitch of 6 mm. The variation of the applied load (kg) of this spring with the extension amount (mm) is shown in Fig. 5. When the slope of the graph is calculated, it is seen that the spring constant is around 1 kg/mm on average. Table legs are also fixed to the concrete floor using similar rubber pads for vibration isolation.

3. RESULTS AND DISCUSSION

Once all the connections were made and the entire experimental setup was assembled, the gain adjustment of the servo valve was performed, and the hydraulic pump, which would pressurize the hydraulic oil, was started. The desired load value was entered into the software. It was observed that the flexible spring compressed proportionally to this positive value. Disturbance inputs were then applied to the system from the user interface defined on the computer via the keyboard. In other words, one of the pistons was moved back and forth. During these back-and-forth movements, it was noticed that the distance between the two ends of the spring remained almost constant, meaning the spring was subjected to the same force value. This observation confirms that the objective of the experiment was achieved.

Finally, the extension and compression amount of the spring corresponding to the entered reference load (desired load) values were recorded. The graphs of these

measurement values are shown in Fig. 6a and Fig. 6b. In the second stage of the experiment, sinusoidal disturbance inputs were applied to the system, and it was observed that, similarly, the distance between the two ends of the spring remained approximately unchanged. However, when the frequency of the disturbance input was increased to around 8-10 Hz, the distance between the two ends began to deviate. Increasing the amplitude further accentuated this deviation, making it more evident.
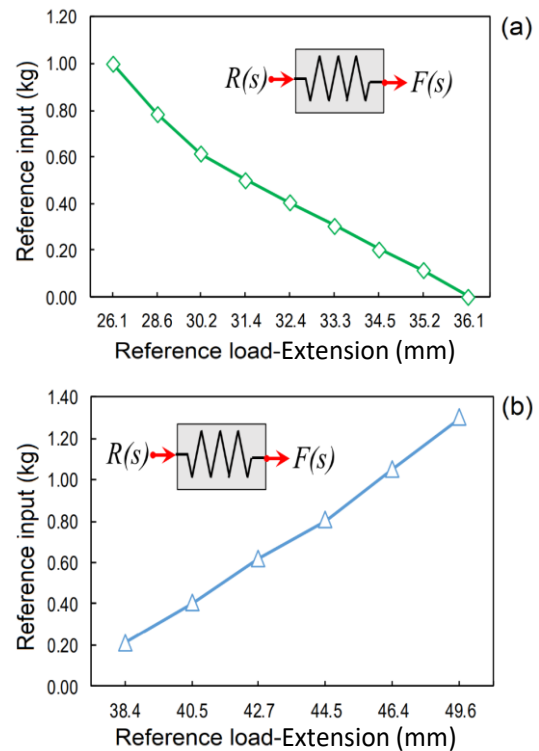
Figure 6. Variation of reference input load with the amount of (a) compression and (b) extension

In this study, as mentioned in the previous section, the aim was to control an analog hydraulic system using a digital computer. Thus, the system under investigation can be divided into two main parts. The first part comprises the analog system, including the servo valve, cylinder, load, servo amplifier, and LVDT. The second part encompasses the digital system, incorporating the reference source, memory elements, sampling switch, and the computer and converter card responsible for the control process. The relationship between these components and their interactions can be summarized as shown in Fig. 7, represented as a schematic and block diagram.
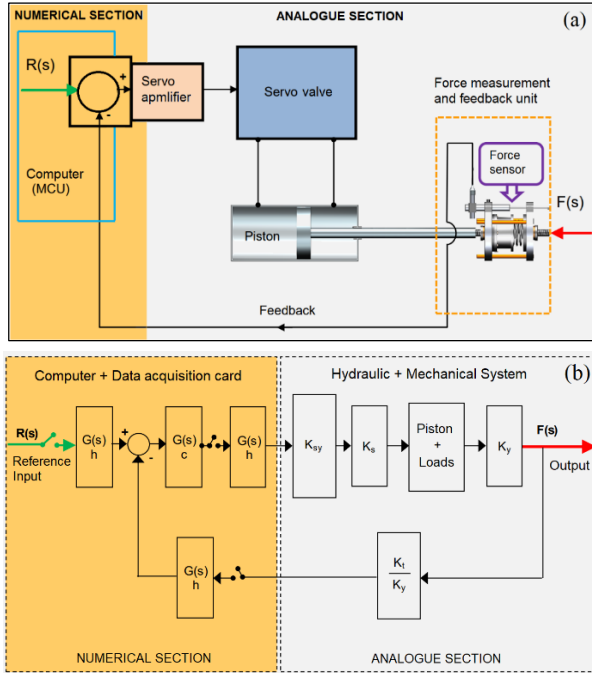
Figure 7. The system (a) components and (b) block diagram

The block diagram, which includes the information flow and variables between the elements that make up the system, is shown in Fig. 8. The operation of the system is as follows: At any "*t*" moment, the transducer output is closed with the switch of the analog input channel and the current position value is measured as voltage. The reference entry can be entered numerically from the computer's memory or from the keyboard. As a result of these operations, position (Load) and reference information are converted into digital. The computer calculates the error numerically by comparing this numerical information it has stored in its memory. A digital command signal is prepared by the computer after this error is passed through the processes of the desired control types. The command signal obtained is converted into an analog signal with the digital/analog converter integrated into the computer and sent to the servo amplifier. This signal is obviously an electrical voltage. The computer keeps this command signal value constant until the next cycle through the register circuits on the control card. The servo amplifier driven by the electric motor drives the torque motor of the servovalve by creating an output current in the order of mA according to the input voltage and the setting of the gain button on it. The servo valve driven by the torque motor ensures that the pressurized oil goes to the hydraulic cylinder. With the movement of the piston, the position of the load changes and the control cycle is thus completed. The computer begins the second cycle by again measuring the transducer output. Unless an external intervention comes, these processes continue continuously. This cycle can be repeated between 250 and 2000 times per second, depending on different programs and computers. The modeling of the analog part consists of servovalve, driving piston and mass-spring system as shown in Fig.

8. Fig. 9 shows the hydraulic part formed by servovalve, piston and external loads. In this system, the servo valve is fed with hydraulic fluid at constant pressure Ps. The torque motor driven by the current signal from the servo amplifier drives the vane-nozzle type first valve stage, and the hydraulic output of the first valve stage drives the second valve stage.

Although a feedback on/off switch has been placed in the block diagram (see in Fig. 7), in experiments, continuous feedback control was applied. Otherwise, it was predicted that the high-amplitude oscillations of the loaded pistons could damage the force sensor designed and produced for these operations.
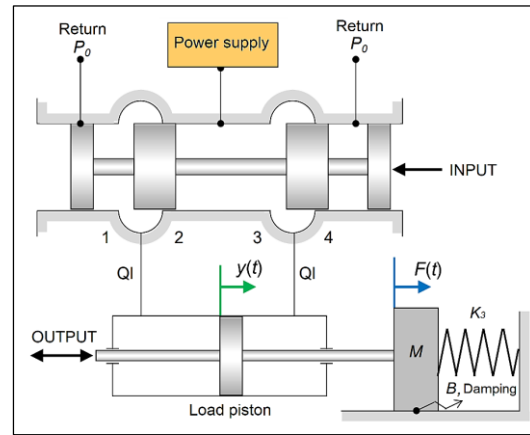
Figure 8. Four-way servovalve, cylinder and load group schematic diagram [3, 5, 13]

If the servovalve pulley is in the position shown in the figure, the orifices (1) and (3) are open, the orifices (2) and (4) are closed. Since the right side of the driving piston depends on the source pressure and the left side depends on the return pressure, the piston moves to the left. If the spool is slid far enough to the left, orifices (2) and (3) are closed; Orifices (2) and (4) are opened. In this new position, the piston moves to the right. Thanks to these synchronized movements, the servovalve implements follow-up control.

Examining the dynamic characteristics of the servo valve and load in proximity to their operational equilibrium involves the use of linearized foundational equations. To begin, the valve's behavior is encapsulated in the following depiction [11, 13-17, 20-23]:

$$Q_L = K_h x - K_2 P_L \tag{1}$$

Where, Q_L, load flow rate, K_h, valve gain at the operating point, K_2, load-pressure sensitivity of the second stage valve, P_L is loading pressure and x means flapper opening. The transfer function between input current and piston position versus spool position dynamics:

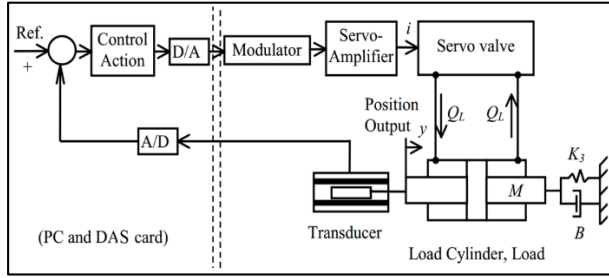$$\frac{X(s)}{I(s)} = \frac{K_h \omega_n^2}{s^2 + 2\xi\omega_n s + \omega_n^2} \tag{2}$$

Figure 9. System structure [5]

Load flow:

$$Q_L = A\dot{y} + \frac{1}{2}\left(\frac{V}{\beta} + K'_e\right)\dot{P}_L + C_2 P_L \qquad (3)$$

Here, the first derivative of load piston position is denoted by $\dot{y}$, A means load piston area, bulk modulus of hydraulic fluid is denoted by β, half-cylinder volume is denoted by V, structural compliance coefficient K'_e, load pressure variation $\dot{P}_L$ and leakage coefficient is denoted by C_2. If the equation of motion of the cylinder-valve subsystem is written, according to Newton's first law:

$$M\ddot{y} + B\dot{y} + K_3 y - F_e = P_L A \qquad (4)$$

In the Eq (5), M is piston mass, B is loading damping coefficient, F_e is disturbance force and K_3 means load spring coefficient. In this case, the transfer function between the servo valve input current (i) and load piston position (y) is found as follows when the values are put in the following expression:

$$\frac{Y(s)}{I(s)} = G(s) = \frac{K_h \omega_n^2}{(s^2 + 2\xi\omega_n s + \omega_n^2)(E_3 s^3 + E_2 s^2 + E_1 s + E_0)} \qquad (5)$$

Here the coefficient of E_0 to E_3 can be written as follows:

$$E_3 = \left[\frac{M}{2A}\left(\frac{V}{\beta} + K'_e\right)\right],$$

$$E_2 = \left[\frac{B}{2A}\left(\frac{V}{\beta} + K'_e\right) + \frac{M}{A}(C_2 + K_2)\right],$$

$$E_1 = \left[\frac{K_3}{2A}\left(\frac{V}{\beta} + K'_e\right) + A + \frac{B}{A}(C_2 + K_2)\right],$$

$$E_0 = \left[\frac{K_3}{A}(C_2 + K_2)\right]. \qquad (6)$$

Upon substituting conventional physical parameters into the aforementioned equations, it becomes apparent that Equation (5)'s denominator encompasses a third-order term featuring two complex conjugate roots and a singular real root. The equilibrium state, designated as y_{ss}, representing the load position in reaction to a consistent current input, i_{ss}, can be derived from Equation (5) in the following manner.

$$\frac{y_{ss}}{i_{ss}} = \frac{K_h}{E_0} = \frac{AK_h}{K_3(C_2 + K_2)} \qquad (7)$$

The provided expression implies that effective control of the load position is contingent upon a non-zero load spring rate, K_3. When K_3 is set to zero, the system shifts its focus to regulating the load velocity. Under such conditions, the corresponding transfer function ($G_V(s)$) governing the relationship between the input current and load velocity can be articulated as follows:

$$\frac{V(s)}{I(s)} = G_V(s) = \frac{K_h \omega_n^2}{(s^2 + 2\xi\omega_n s + \omega_n^2)(E_3 s^2 + E_2 s + E_1)} \qquad (8)$$

Hence, from the given transfer function, the steady-state relationship between the input current and load velocity can be obtained as below:

$$\frac{v_{ss}}{i_{ss}} = \frac{K_h}{E_1} \qquad (9)$$

In their innovative work, Keleş and Ercan developed a novel numerical simulation approach to determine the step response of the closed-loop system, as illustrated in Fig. 9. This simulation method operates in discrete time intervals, symbolized as Δt, which serve as sampling periods (greater than the pulse period). During each step (j^{th} step), the input current is assumed to remain constant, i.e., $i(t) = ij$. By utilizing the values of $r(t)$ and $y(t)$ from the previous step, denoted as rj-1 and yj-1 respectively, in conjunction with a relevant relationship, the precise value of ij is computed [5].

$$i_j = K_p(r_{j-1} - K_t r_{j-1}) \qquad (10)$$

Examine the voltage input, $u(t)$, fed into the demodulator from the PC. In instances where $u(t)$ maintains a constant value, r_0, the modulated signal, $u_m(t)$, displays periodic characteristics aligned with the frequency of the modulating pulse, as illustrated in Fig. 10. To ascertain the center-shift time, denoted as 'a_j' a key parameter governing this temporal aspect can be deduced using the following expression:

$$a_j = \frac{Ti_j}{H} \qquad (11)$$

The time a_j for the jth step, which corresponds to the shift of the center, is determined by Eq. (11) as below.
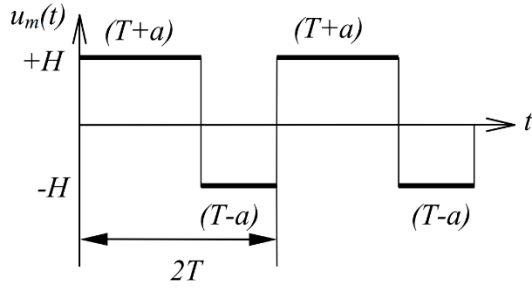
Figure 10. The pulse-width modulated representation of a constant signal [5]

As a result of a series of Laplace transformations and inverse transformations to be applied to the system equations, an equivalence between the piston position $Y(s)$ and the system parameters is obtained, given by Eq. (12):

$$Y(s) = \frac{\frac{K_h \omega_n^2}{E_3}}{(s^2 + 2\xi\omega_n s + \omega_n^2)\left(s^3 + \frac{E_2}{E_3}s^2 + \frac{E_1}{E_3}s + \frac{E_0}{E_3}\right)}$$

$$\times \left[\frac{A_0}{s} + \sum_{n=1}^{\infty}\left[A_n \frac{s}{s^2 + \left(\frac{n\pi}{T}\right)^2} + B_n \frac{\left(\frac{n\pi}{T}\right)}{s^2 + \left(\frac{n\pi}{T}\right)^2}\right]\right]$$

$$+ \frac{\begin{pmatrix}(s^4 + A_4 s^3 + A_3 s^2 + A_2 s + A_1)y(0) \\ +(s^3 + A_4 s^2 + A_3 s + A_2)y'(0) \\ +(s^2 + A_4 s + A_3)y''(0) + (s + A_4)y'''(0) + y''''(0)\end{pmatrix}}{(s^2 + 2\xi\omega_n s + \omega_n^2)\left(s^3 + \frac{E_2}{E_3}s^2 + \frac{E_1}{E_3}s + \frac{E_0}{E_3}\right)}$$

(12)

In this context, the coefficients E_3, E_2, E_1, and E_0 are defined as mentioned previously, based on Eq. (6). As for the coefficients A_4, A_3, A_2, A_1, and A_0, they are defined as

follows:

$$A_4 = \left(\frac{E_2}{E_3} + 2\xi\omega_n\right), \quad A_3 = \left(\frac{E_1}{E_3} + \frac{E_2}{E_3}2\xi\omega_n + \omega_n^2\right),$$

$$A_2 = \left(\frac{E_0}{E_3} + \frac{E_1}{E_3}2\xi\omega_n + \frac{E_2}{E_3}\omega_n^2\right),$$

$$A_1 = \left(\frac{E_0}{E_3}2\xi\omega_n + \frac{E_1}{E_3}\omega_n^2\right), \quad A_0 = \left(\frac{E_0}{E_3}\omega_n^2\right).$$

(13)

Rigid connecting lines are employed to establish a connection between the valve and the actuator. The corresponding parameter values for both the actuator and load can be found in Table 1, offering a comprehensive overview of the associated metrics.

The additional specifications provided by the valve manufacturer include the following:

ω_n=1256.64 (rad/s), ξ = 0.7 and I_{max}=13.25 mA

To provide power to the system, pressure-compensated hydraulic feed with a flow rate of 60 (l/min) and a supply pressure of 100 (bar) was utilized. Experiments demonstrated remarkable stability at both pulse and reference input frequencies, as the pump and servo valve exhibited a seamless and harmonious integration. During testing, no visible fluctuations were detected, indicating that these components did not perform harmoniously.

When all these parameters are applied to the system and run, the time changes of the piston position for the unit step input are obtained. In the experiments, it has been observed that the valve flow rate remains constant when the driving current is 13.6 mA or greater. In order to prevent this situation, a step test input was applied to prevent the valve from reaching the maximum opening, especially at high gains.

Table 1. The parameter values related to the actuator and loads [5]

Parameters and values									
A	*V*	C_2	K'_e	*B*	K_3	*B*	*M*	K_h	K_2
(m^2)	(m^3)	(sPa)	(m^3/Pa)	(Pa)	(N/m)	(N/m/s)	(kg)	(m^3/smA)	(m^3/sPa)
2.69E4	3.43E-5	0	0	1.72E9	0	295	0.85	2.48E-6	1.72E-12

System responses including the saturated state of the valve during the experiments are shown in Fig. 11 according to the unit step input. Keleş and Ercan, in their study using the same experimental set, used four different pulse frequency values to experimentally determine the step response of the closed-loop system [5].

The variation of the piston positions with time according to the unit step signal input is shown in Fig. 11(a)-(d) for each of the four different frequency values, respectively. The data presented here illustrates the behavior of the

closed-loop system in response to a step input, with a specified gain of K_p=20. The depicted curves reveal that oscillations occurring at the pulse frequency coincide with the system responses. The time constants observed in this context vary within the range of 0.065 to 0.075 seconds. Analysis of the results indicates that the theoretically determined final mean values exhibit a maximum deviation of 11% from their experimentally determined counterparts. Notably, disparities between theoretical and experimental time constants span from
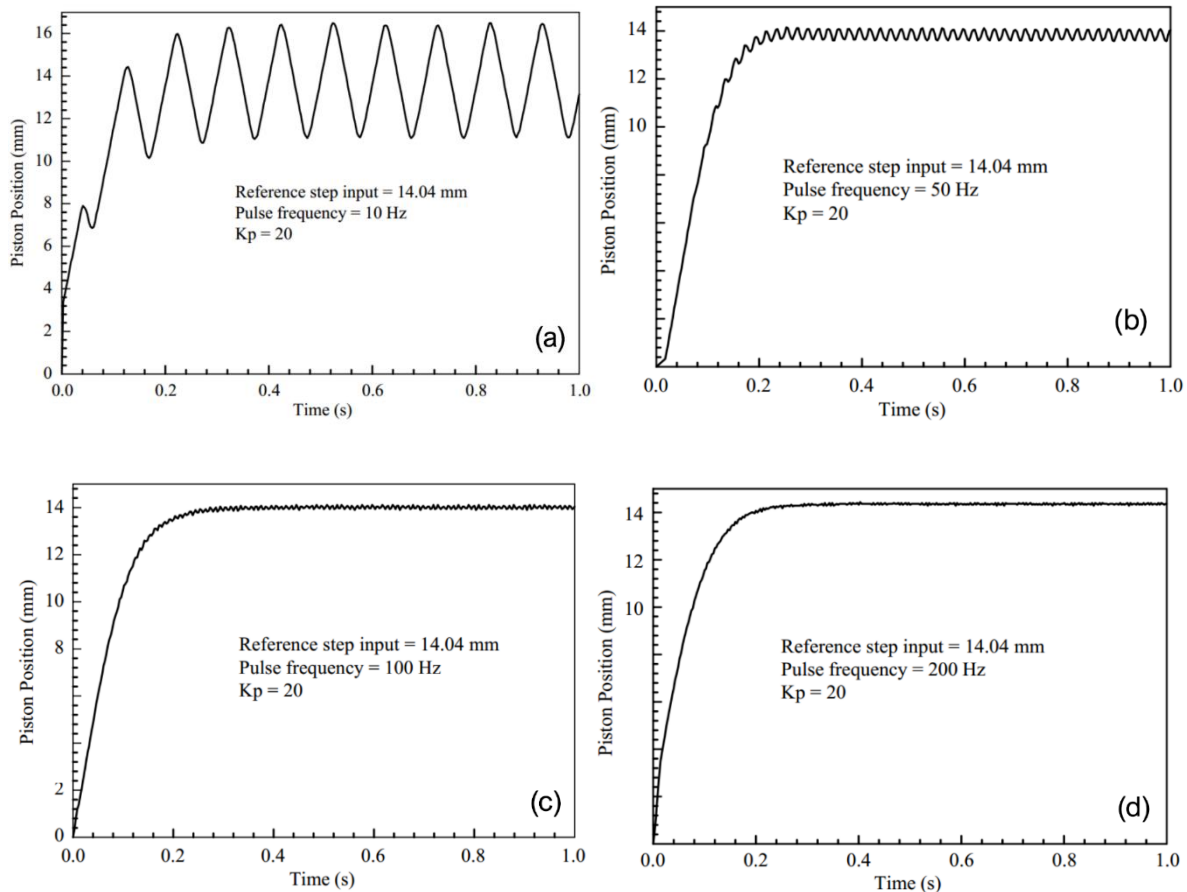
Figure 11. Step response of the pulse-width modulated closed loop system for (a) 10, (b) 50, (c) 100 and (d) 200 Hz pulse frequency [5].

1.4% to 50%. Interestingly, it appears that the differences between theoretical and experimental outcomes become more pronounced when dealing with lower proportional gains.

To showcase or illustrate the concept, it is imperative to the effectiveness of pulse width modulation in attenuating hold-slip motion for heavy loads, a closed loop system was implemented and a small ramp reference input was added. This input simulated a slope matching a load rate of 20 mm/min. A series of experiments were performed with pulse frequencies of 10, 50, 100 and 200 Hz to evaluate the performance of the system. The results, even at such low load velocities, showed that stick-slip did not occur. In the system shown in Fig. 11(a), with a reference step value of 14.04 mm and a pulse frequency of 10 Hz, oscillations were observed to be marginally stable within a position band of approximately 6 mm after about 0.2 seconds. Figure 11(b) shows that the oscillation amplitude was slightly more stable within a narrower position band (approximately 1.5 mm), and the position reached the 14 mm level after about 0.2 seconds, continuing with very small amplitude oscillations at that level. The system exhibited the highest stability with step signals of 200 Hz frequency, as clearly seen in Fig. 11(d), reaching the 14.04 mm value with much lower oscillations compared

to the 100 Hz frequency, and becoming parallel to the time axis after about 3 seconds. In this study, the responses of the servovalve-piston subsystem are shown in Fig. 12 for three different gains in proportional control (P) with a unit step input. The servovalve used in the experiments reaches saturation after reaching the maximum drive current (approximately 13.6 mA). This value corresponds to an average position of approximately 14 mm (See Fig. 12).
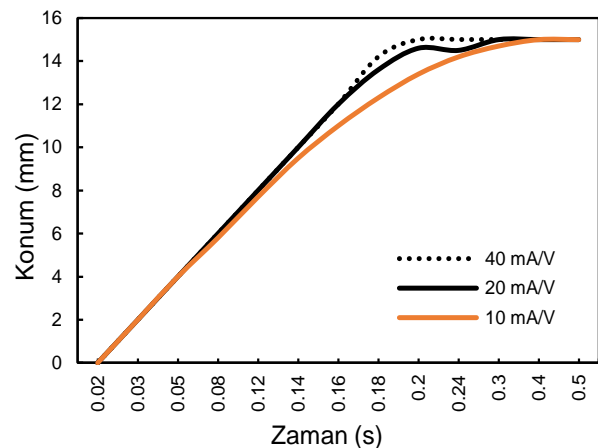
Figure 12. Response of servovalve-piston subsystem to unit step input for P control

When the entire system is operated, significant fluctuations occur in the LVDT attached to the pistons as they are moved back and forth until the system reaches its equilibrium position as shown in Fig. 13. As the system approaches a steady state, the magnitude of the oscillations decreases with time, as in some other studies [12, 24, 19-32]. It is observed that the system reaches the equilibrium position more quickly at higher frequencies. The signal processing frequency, shown in blue, exhibits the highest amplitude oscillation at around 50 Hz. At 100 Hz (shown in Fig. 13 as red color), it reduces from 4 mm amplitude to nearly zero, and at approximately 200 Hz (shown in Fig. 13 as green color), it reaches a similar zero position from an amplitude of approximately 2.2 mm in comparable time durations.

When the region enclosed by the dashed line marked with an arrow in the graph (Fig. 13) is taken under the lens, the graph in Fig. 14 is obtained.
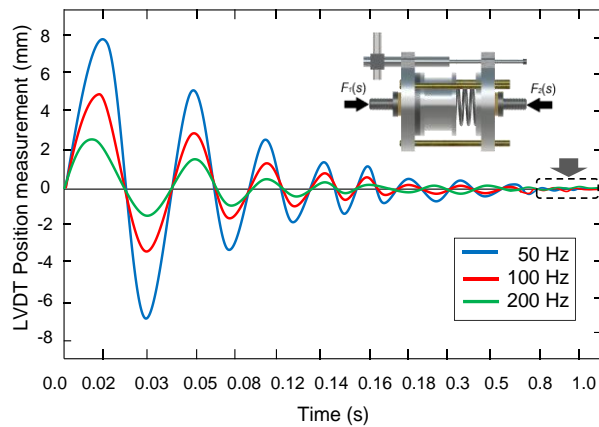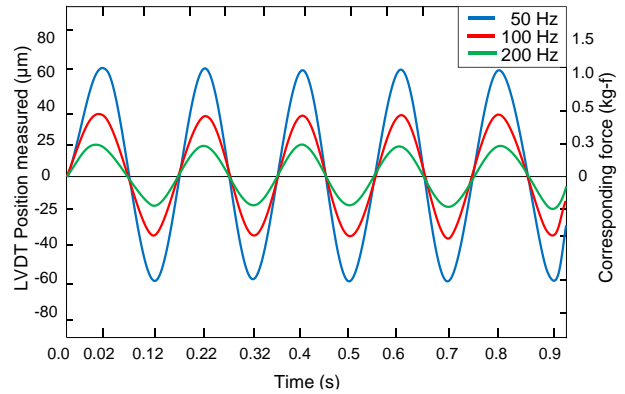

Figure 13. Variation of the position measured from the sensor with time for three different pulse frequencies

It becomes marginally stable approximately 8 seconds after power is applied to the system. Comparison chart according to three different frequency values shown at Fig.14. It was measured from the computer that while the system oscillates at a frequency of 50 Hz in a range of about 120 micrometers, it oscillates in a range of about 50 µm towards 200 Hz. This value hovers at a margin of 80 µm at 100 Hz (See Fig. 14).

The force values corresponding to the displacements measured during the experiments are shown on the right side of the graph in kg-f units calculated by multiplying the displacements by a coefficient on the computer. According to the graph, a displacement of 60 µm corresponds to approximately 1 kg-f of force. A commercial load cell can be added to the system to calibrate the system and verify its accuracy. Calibration is performed by comparing the measured force values and the calculated force values by means of the commercial load cell included in the system.

With this approach, the sensor designed within the scope of this study can be easily adapted as an active suspension

system for high-speed trains or road vehicles with necessary design modifications, as shown in Fig. 15.

Figure 14. Marginally stability region of the position measured from the sensor with time for three different pulse frequencies

Unlike known ordinary suspension systems [33], in the adapted active suspension system an electro-servo hydraulic piston is placed between the vehicle chassis ($F_1(s)$) and the sensor, and at the other end of the piston, a ground-wheel reference ($F_2(s)$) simulating the disturbance input is applied. Moreover, by integrating an embedded computer into the system, the suspension stiffness can be adjusted by the user or automatically based on different road conditions, making it a significant improvement in terms of adaptability.
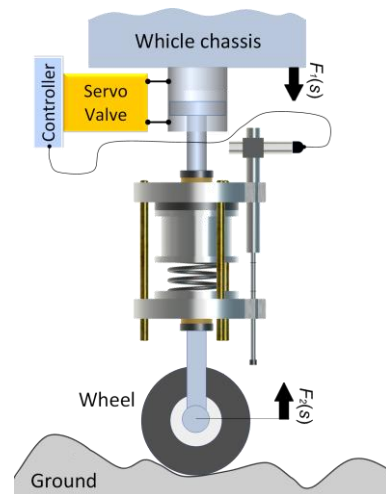
Figure 15. Adaptation of the servo-force mechanism as an active suspension

The similar solution can also be seen in the work by Tseng and Hrovat [17] where they developed a semi-active suspension system. They investigated a 2-degree-of-freedom (2 DOF) quarter-car model equipped with an actuator that generates forces between the vehicle body/sprung mass and wheel/unsprung mass. With their developed control and integrated suspension system, they were able to achieve a certain level of vibration isolation.

Our study demonstrates that a pulse width modulation (PWM) analog hydraulic position control system, using a force sensor developed by digital electro-hydraulic servo systems, can be successfully used for precise force control over the position. It can be concluded that the pulse frequency is a crucial parameter for pulse width-modulated hydraulic systems based on these results. To minimize marginal oscillations in the system response, the pulse frequency should be chosen sufficiently high. At high frequencies, the entire system quickly reaches equilibrium, and the desired force is applied to the sensor placed between the pistons. However, at very low frequencies, around 10-15 Hz for instance, the system fails to reach complete equilibrium, leading to continuous high-amplitude oscillations. It was observed that calibrating the LVDT before measurements and isolating the working environment from internal and external vibrations by placing the table legs and piston bottoms on rubber (silicone rubber) pads yielded better results.

Certainly, it is considered that the application of other control methods such as PID, adaptive control, robust control, and others to this developed system could yield better results.

Moreover, the research findings present a versatile hydraulic system that boasts seamless adaptability to pneumatic applications. Through a simple manipulation of control coefficients, the system can be swiftly transformed into a pneumatic counterpart, offering a dynamic solution for scenarios demanding reduced power consumption. This groundbreaking feature not only enhances the system's efficiency but also opens up a realm of possibilities for its implementation across various industries seeking resource-efficient alternatives.

4. CONCLUSION

The work carried out has led to the design, modeling and manufacturing of a new cost-effective servo-controlled active force sensor. The operation and behavior of the system were investigated theoretically and practically through performance experiments. Research has shown that a pulse-width modulated (PWM) digital hydraulic position control system can be successfully used for force control over position, achieved through a force sensor developed by digital electro-hydraulic servo systems. Especially at high pulse frequencies such as 200 Hz, the response of the system was found to exhibit negligible marginal oscillations, providing much more stable and precise force control. However, at low frequencies around 10-15 Hz, the system did not reach full equilibrium, resulting in sustained high amplitude oscillations. The designed force sensor can be adapted for use as an active suspension system for high-speed trains or road vehicles with necessary design modifications. It is predicted that such active servo force mechanisms are based on the impact frequency as the basic parameter and it is very important to isolate the working environment from internal and external vibration effects in order to obtain more stable and precise results. Overall, the study

demonstrated the successful implementation of a pulse-width modulated hydraulic control system using a digital electro-hydraulic servo system to achieve position-based force control. The results gained from this research could be valuable for the development of active suspension systems and other applications where force control is paramount. The research reveals a highly adaptable hydraulic system that can easily convert to a pneumatic system through control factor adjustments. This transformation provides a dynamic solution for power-efficient applications and opens up new application possibilities in various industries.

DECLARATION OF ETHICAL STANDARDS

The author of this article declares that the materials and methods used in his studies do not require ethics committee permission and/or legal-specific permission.

AUTHORS' CONTRIBUTIONS

Kemal YAMAN: Perofrmed the experiments and analyse the results.

CONFLICT OF INTEREST

There is no conflict of interest in this study.

REFERENCES

[1] Ogata, K., "Automatic Control**",** ***Prentice Hall, Englewood Cliffs***, (1990).

[2] Ercan, Y., "Mühendislik sistemlerinin modellenmesi ve dinamiği", ***Gazi Üniversitesi Yayınları*** No: 179, (1992).

[3] Ercan, Y., "Akışkan gücü ve kontrolü***", Gazi Üniversitesi Yayınları***, No. 206. (1995).

[4] Dindorf R., P. Wos, "Force and position control of the integrated electro-hydraulic servo-drive", ***20th International Carpathian Control Conference (ICCC),*** Krakow-Wieliczka, Poland, 1-6, (2019). doi: 10.1109/CarpathianCC.2019.8765986.

[5] Keles O., Ercan Y., "Theoretical and experimental investigation of a pulse-width modulated digital hydraulic position control system", ***Control Engineering Practice***, 10: 645–654, (2002).

[6] Usta Y., "Sayısal bir hidrolik pozisyon kontrol sistemi geliştirilmesi ve denenmesi" ***Yüksek Lisans Tezi*** G.Ü. Fen Bilimleri Enstitüsü, Ankara, (1991).

[7] Priyandoko G., Mailah, M., Jamaluddin H., "Vehicle active suspension system using skyhook adaptive neuro active force control", ***Mechanical Systems and Signal Processing***, 23: 855–868, (2009).

[8] Fateh M.M., Alavi S.S., "Impedance control of an active suspension system", ***Mechatronics***, 19: 134–140, (2009).

[9] Wu J., Huang Y., Song Y., Wu D., "Integrated design of a novel force tracking electro-hydraulic actuator", ***Mechatronics***, 62: 102247, (2019).

[10] Li J.Y., Shao J.P., Wang Z.W., Wu B., Han G.H., "Study of electro-hydraulic force servo control system based on fuzzy control, *IEEE Xplore, IEEE International Conference on Intelligent Computing and Intelligent Systems*, Shanghai, pp. 688-693, (2009). doi: 10.1109/ICICISYS.2009.5358308.

[11] Li J.Y., Zhongwen, J. S., WU W. Bo, G. Han, "Study of the electro-hydraulic load simulator based on double Servo Valve Concurrent Control", *The Ninth International Conference on Electronic Measurement & Instruments (ICEMI 2009)*, Harbin University of Science and Technology, China. (2009).

[12] Chen L., Jiang J., Gao W., Wang C., Xu W., Ai C., Chen C., "Position control for a hydraulic loading system using the adaptive backsliding control method", *Control Engineering Practice,* 138: 105586, (2023).

[13] Fu S., Lu S., Kai G., "Characteristics and Control Technology Research of Three-stage Electro-hydraulic Servo Valve", *Journal of Applied Science and Engineering Innovation*, 2(2): 43-45, (2015).

[14] Feng H., Song Q., Ma S., Ma W., Yin C., Cao D., "A new adaptive sliding mode controller based on the RBF neural network for an electro-hydraulic servo system", *ISA Transactions*, 129: 472–484, (2022).

[15] Coşkun M.Y., İtik M., "Intelligent PID control of an industrial electro-hydraulic system", *ISA Transactions*,

(Article in press), (2023),
https://doi.org/10.1016/j.isatra.2023.04.005

[16] Yang G., Jao J., "Multilayer neuroadaptive force control of electro-hydraulic load simulators with uncertainty rejection", *Applied Soft Computing*, 130: 109672, (2022).

[17] Çakan A., Botsalı F.M., Önen Ü., "Kalyoncu M., Modeling of electro-hydraulic servo system using the BEES algorithm", *Konya Journal of Engineering Sciences*, 10(1): 1-10, (2022).

[18] Gao B., Guan H., Shen W., Ye Y., Application of the gray wolf optimization algorithm in active disturbance rejection control parameter tuning of an electro-hydraulic servo unit, *Machines*, 10: 599, (2022).

[19] Özkan Y., "Quick basic 4.50", *Alfa kitabevi*, (1994).

[20] Ahmad, X. Ge, Q. -L. Han and Z. Cao, "Dynamic Event-Triggered Fault-Tolerant Control of Vehicle Active Suspension Systems," *IECON 2020 The 46th Annual Conference of the IEEE Industrial Electronics Society*, Singapore, 2020, pp. 4889-4894.

[21] Hsiao C.-Y., Wang Y.-H., "Evaluation of ride comfort for active suspension system based on self-tuning fuzzy sliding mode control", *International Journal of Control, Automation and Systems*, 20(4): 1131-1141, (2022).

[22] Kumar S., Medhavi A., Kumar R. Mall P.K., "Modeling and analysis of active full vehicle suspension model optimized using the advanced fuzzy logic controller", *International Journal of Acoustics and Vibration*, 27(1): 26-36, (2022).

[23] Chen H.-M., Yang G.-W., Liao C-C., "Precision Force Control for an Electro-Hydraulic, Press Machine", *Smart Science*, 2(3): 132-138 (2016).

[24] Shao J., Li J., Wang Z., Han G., "Research on electro-hydraulic load simulator based on building model of flow press servo valve", *Advanced Materials Research,* 129(131): 213-217, (2010).

[25] Ahmed A.S., Ali A.S., Ghazaly N.M., Abd-el Jaber G.T., "PID controller of active suspension system for a quarter car model", *International Journal of Advances in Engineering & Technology*, 8(6): 899-909 (2015).

[26] Jones B.E., "Feedback in instrument and its applications", *Mc Graw-Hill*, New York. (1979).

[27] Tseng H.E., Hrovat D., "State of the art survey: active and semi-active suspension control", *Vehicle System Dynamics*, 53(7): 1034-1062, (2015).

[28] Raghavendra D. R., *"Electrohydraulic Servo Systems: Applications, Design and Control",* Springer Nature, (2021).

[29] Fan Y., Shao J., Sun G., Shao X., "Proportional–Integral–Derivative controller design using an advanced lévy-flight salp swarm algorithm for hydraulic systems", *Energies*, 13: 459, (2020).

[30] Wu L., Zhao D., Zhao X., Qim Y., "Nonlinear adaptive back-stepping optimization control of the hydraulic active suspension actuator", *Process*, 11: 2020, (2023).

[31] Adıgüzel F., "Doğrusal karesel regülatör ve ileri beslemeli kontrol yöntemi ile otonom araçlar için kooperatif uyarlamalı hız kontrol sistemi", *Journal of Polytechnic*, DOI: 10.2339/politeknik.1170311, (2022).

[32] Ünal A., Yaman K., Okur E., Adlı M.A., "Design and implementation of a Thrust Vector Control (TVC) test system", *Journal of Polytechnic*, 21(2): 487-505, (2018).

[33] Putgül Y., Altıparmak D., "Taşıt süspansiyon sistemi çeşitleri ve ön düzen geometrisine etkileri", *Journal of Polytechnic*, 19(2): 195-202, (2016).